

# The critical role of water at the gold-titania interface in catalytic CO oxidation

**Johnny Saavedra,<sup>1</sup> Hieu A. Doan,<sup>2</sup> Christopher J. Pursell,<sup>1</sup> Lars C. Grabow,<sup>2\*</sup> Bert D. Chandler<sup>1\*</sup>**

<sup>1</sup>Department of Chemistry, Trinity University, San Antonio, TX 78212-7200, USA. <sup>2</sup>Department of Chemical and Biomolecular Engineering, University of Houston, Houston, TX 77204-4004, USA.

\*Corresponding author. E-mail: bert.chandler@trinity.edu (B.D.C.); grabow@uh.edu (L.C.G.)

**We provide direct evidence of a water-mediated reaction mechanism for room-temperature CO oxidation over Au/TiO<sub>2</sub> catalysts. A hydrogen/deuterium kinetic isotope effect of nearly 2 implicates O-H(D) bond breaking in the rate determining step. Kinetics and in-situ infrared spectroscopy experiments showed the coverage of weakly adsorbed water on TiO<sub>2</sub> largely determines catalyst activity by changing the number of active sites. Density functional theory calculations indicated that proton transfer at the metal-support interface facilitates O<sub>2</sub> binding and activation; the resulting Au-OOH species readily reacts with adsorbed Au-CO, yielding Au-COOH. Au-COOH decomposition involves proton transfer to water, and was suggested to be rate determining. These results provide a unified explanation to disparate literature results, clearly defining the mechanistic roles of water, support OH groups, and the metal-support interface.**

The interactions between transition metal nanoparticles and their metal-oxide supports are often critical for heterogeneous metal nanoparticle catalysts (1). However, the roles of the species involved are often not well understood, especially for supported Au catalysts, which are active for selective hydrogenations (2, 3), oxidations (3–5), and the water-gas shift (WGS) reaction (3, 6). Several factors have been suggested for the exceptionally high activity of Au catalysts, including quantum size effects (7), particle geometry (8, 9), and under-coordinated Au atoms (10–12).

Oxygen activation at the metal-support interface is widely regarded as the key step in room-temperature CO oxidation (13–17), but substantial debate remains regarding the nature of the active site (9, 12, 17–23). Experimental studies indicate that materials lacking OH groups are inactive (24, 25), yet, the dominant mechanistic models vary in the suggested role of support OH groups and generally highlight the possible role of oxygen vacancies (16, 17, 22–24, 26). Computational models also have not indicated a clear mechanistic role for the support OH groups, and isotope labeling studies indicate that CO and O<sub>2</sub> react without incorporating oxygen from the support (21, 27). Perhaps most importantly, as Fig. 1A shows, water dramatically increases catalytic activity (20, 21, 26, 27), yet only one proposed mechanism suggests a direct potential role for water (21).

We performed an experimental and computational study to better understand how water, surface hydroxyls, and the metal-support interface interact during CO oxidation over Au/TiO<sub>2</sub> catalysts. The surface water and hydroxyl groups of a commercial Au/TiO<sub>2</sub> catalyst were deuterated in-situ with flowing D<sub>2</sub>O/N<sub>2</sub> (SM 3.1–3.2). The exchanged catalyst was then flushed with N<sub>2</sub> to remove excess D<sub>2</sub>O. Under these conditions, we measured a large kinetic isotope effect (KIE,  $k_H/k_D = 1.8 \pm 0.1$ , Fig. 1B), consistent with a primary KIE, indicating O-H(D) bond cleavage in the rate-determining step (RDS). Previous studies on Au/Al<sub>2</sub>O<sub>3</sub> catalysts (21, 28) found almost no rate difference ( $k_H/k_D \approx 1$  to 1.2) upon switching H<sub>2</sub>O for D<sub>2</sub>O in the feed and concluded that an equi-

librium isotope effect might be involved (21). However, adding 700 Pa H<sub>2</sub>O/D<sub>2</sub>O to the feed reduced the KIE to 1.4. This change was reversible: 60 min after removing H<sub>2</sub>O/D<sub>2</sub>O from the feed, the KIE approached the original value (Fig. 1C). The large KIE under relatively dry conditions indicates that water or support OH must be involved in the reaction mechanism and that O-H(D) bond cleavage occurs in a kinetically important step. Further, the reaction is subject to saturation kinetics, with added water affecting the kinetics of the RDS.

We explored potential mechanistic roles of O-H bonds with density functional theory (DFT) studies using a 10-atom gold nanocluster residing on 4 layers of TiO<sub>2</sub>(110) support. Unlike previous studies, our computational model (SM 2.5–2.6) includes both support OH groups and adsorbed water (13, 14, 18, 29). This model substantially simplifies the real system, using a small Au cluster and a single water molecule to represent 3 nm particles and multiple water molecules. DFT calculations can provide substantial insight into likely elementary reaction

steps, but need to be interpreted in the context of the more complex real system.

The H<sub>2</sub>O molecule adsorbed on a bridging OH group at the metal-support interface through hydrogen bonding interactions; this adsorption motif was ~1.0 eV more stable than adsorption on the Au cluster and ~1.4 eV more stable than adsorption on a bridging OH group away from the interface (SM 6.1). Although we studied several O<sub>2</sub> adsorption and activation pathways (Fig. 2, SM 6.2–6.3), we did not find an intermediate species with O<sub>2</sub> bound only to Au atoms near the metal-support interface. In all cases, an essentially barrier-free proton transfer lowered the overall energy of the system, generating H<sub>2</sub>O<sub>2</sub><sup>\*</sup> or \*OOH (Fig. 2; “\*” references species adsorbed to Au). Once \*OOH formed, it migrated along the Au particle, allowing atoms near, but not strictly at, the metal-support interface to participate in the reaction.

The KIE and DFT studies indicate proton transfer in a key reaction step, but they do not provide sufficient information to determine if the reaction is initiated by adsorbed water or support OH groups. In-situ infrared spectroscopy was therefore used to quantify these species (SM 4.1) and compare catalyst activity to their relative surface concentrations. The non hydrogen-bonded  $\nu_{OH}$  stretching vibration centered at 3650 cm<sup>-1</sup> is exclusively associated with support OH groups, whereas the  $\delta_{HOH}$  bending vibration centered at 1623 cm<sup>-1</sup> is exclusively due to adsorbed water. There is also a broad band centered around 3400 cm<sup>-1</sup> assigned to  $\nu_{OH}$  for OH groups involved in hydrogen bonding that may have contributions from both water and Ti-OH (IR analysis in SM 4.1).

Our catalysis studies do not indicate a direct role for support OH groups in the reaction mechanism. Gentle drying with flowing N<sub>2</sub> (Table 1 and Fig. 3A) only removed water and had little effect on the support OH bands. Catalytic activity, however, dropped by an order of magnitude, indicating that adsorbed water, not support OH, is the key proton donor. Further, a constrained *ab-initio* thermodynamic analysis (SM 2.6) indicates that the support OH groups at the metal-support interface are thermodynamically unstable relative to gas-phase water under dry condi-

tions, and therefore would be unavailable as proton donors. As water is added to the system, the interfacial support OH groups and weakly adsorbed water are equilibrated and ultimately become indistinguishable.

Several literature mechanisms invoke OH transfer from the support to Au (17, 23) as an elementary step. Our experimental and DFT studies do not support such a step. The calculated barrier for transferring a  $\text{Ti}^{\text{cus}}\text{-OH}$  group to Au ( $E_a = 1.63$  eV, SM 6.5) is too large to be a viable room-temperature pathway. Further, generating  $^{*}\text{COOH}$  from  $^{*}\text{CO}$  and  $^{*}\text{OOH}$  ( $\Delta E = -2.23$  eV,  $E_a = 0.10$  eV) is thermodynamically and kinetically far more favorable than the reaction between  $^{*}\text{CO}$  and  $\text{Ti}^{\text{cus}}\text{-OH}$  ( $\Delta E = 0.60$  eV,  $E_a = 0.72$  eV, SM 6.5).

To quantify the effects of adsorbed water, we performed a series of adsorption, thermogravimetric analysis (TGA), and kinetics experiments. IR spectroscopy showed water adsorption on titania (not on Au, SM 4.1), consistent with DFT calculations (SM 6.1). The adsorption isotherm quasi-saturated around 700 Pa (1.7 wt %, 13 molecules/nm<sup>2</sup>), corresponding to roughly 1.5 monolayers of water on titania, suggesting a bilayer adsorption structure typical for water (30). The reaction rate correlates extremely well with the amount of weakly adsorbed water and the reaction order (1.33, Fig. 3B) is substantially larger than the reaction orders for CO or O<sub>2</sub>, (0.01 and 0.1–0.3, respectively, SM 5.1–5.3).

We further evaluated the reaction kinetics using a Michaelis-Menten (M-M) kinetic model (SM 5.2), which provides quantitative metrics that characterize heterogeneous catalysts (31). This model helps distinguish between changes in the inherent activity of the active site (measured with  $K_R$ —analogous to the conventional  $K_M$ ) and the relative number of active sites (associated with  $v_{\max}$ ). Double reciprocal plots of the O<sub>2</sub> dependence data (Fig. 3C) yield  $K_R$  values that are independent of the water coverage (Fig. 3D), indicating that H<sub>2</sub>O did not affect the inherent reactivity of the active sites. The  $v_{\max}$  values, however, increased linearly with adsorbed water. Since  $K_R$  was essentially constant, this indicates that weakly adsorbed water increased the effective number of active sites rather than changing their inherent reactivity.

Two explanations for increasing the number of active sites are consistent with the DFT studies and recognize the importance of the metal-support interface (9, 12, 18–23). First, if oxygen binding requires protons from weakly adsorbed water, then increasing the water coverage should increase the number of available protons, and facilitate O<sub>2</sub> binding. Second, the DFT studies suggest that  $^{*}\text{OOH}$  can interact with Au atoms that are near, but not strictly at the metal-support interface. As additional Au sites gain access to protons from water, a greater number of O<sub>2</sub>/peroxy binding sites become available. This increase in active site density also argues strongly against O atom vacancies on the support being the active sites for O<sub>2</sub> activation, as surface water would be expected to rapidly fill those vacancies.

The conclusion that support OH groups do not directly participate in the reaction mechanism requires a new model to explain why the support and surface OHs strongly influence CO oxidation activity (13–15, 24, 25). Our results indicate that the support OH groups' primary role is to anchor active water near the Au particle, and possibly help activate it through hydrogen bonding. The relative number of support OHs near Au particles and their ability to anchor enough water to facilitate the reaction may partially explain the strong support effects reported in the literature (3, 17, 22, 23).

While the DFT results for O<sub>2</sub> adsorption are congruent with proton transfer as part of the mechanism, they do not explain the observed KIE. The  $^{*}\text{OOH}$  species have moderate direct decomposition barriers ( $E_a \sim 0.5$  eV, Fig. 2 and SM 6.3). However, CO-assisted  $^{*}\text{OOH}$  activation yielding  $^{*}\text{O}$  and  $^{*}\text{COOH}$  was found to be extremely facile ( $E_a = 0.10$  eV, Fig. 2). This O-OH dissociation barrier is lower than the previously reported barriers for the related CO-assisted O<sub>2</sub>\* dissociation on supported and unsupported Au clusters (10, 13, 14, 18, 32). In stark contrast to the predominant literature opinion (16), the extremely low barriers associat-

ed with this pathway suggest that O<sub>2</sub> activation is quite facile in the presence of water and CO.

To explain the observed KIE and close the catalytic cycle, we explored possible  $^{*}\text{COOH}$  decomposition pathways (SM 6.6); Fig. 4 shows the two most relevant pathways. In the first pathway, the proton is spontaneously transferred from  $^{*}\text{COOH}$  to the co-adsorbed O\* (green,  $\Delta E = -0.27$  eV,  $E_a = 0.0$  eV), leaving  $^{*}\text{OH}$  on the surface after CO<sub>2</sub> desorption. Closing the catalytic cycle requires the direct reaction between  $^{*}\text{OH}$  and  $^{*}\text{CO}$  ( $\Delta E = 0.10$  eV,  $E_a = 0.40$  eV, SM 6.4) to yield  $^{*}\text{COOH}$ , followed by  $^{*}\text{COOH}$  decomposition, which returns the proton and restores the active site. The second pathway is initiated by an endothermic proton transfer from  $^{*}\text{COOH}$  to an adsorbed water molecule (simultaneously transferring a proton to the support) (purple,  $\Delta E = 0.61$  eV;  $E_a = 0.76$  eV), followed by CO<sub>2</sub> desorption. The remaining O\* reacts with  $^{*}\text{CO}$  in a well studied reaction ( $\Delta E = -1.03$  eV;  $E_a = 0.65$  eV, SM 6.4).

These pathways are chemically similar, differing primarily in the order of the steps. The reactions between  $^{*}\text{CO}$  and  $^{*}\text{O}$  or  $^{*}\text{OH}$  have fairly similar barriers, and both pathways also go through the same endothermic  $^{*}\text{COOH}$  decomposition step. This step is the likely RDS because it involves a proton transfer ( $^{*}\text{COOH}$  to water) and has the highest computed activation energy barrier (movie S1). DFT calculations based on this transition state (involving a single water molecule) yielded a calculated KIE of 2.55 (SM 6.7), which represents an upper limit to the experimentally determined KIE at low water coverage. The predicted lower limit of the equilibrium isotope effect associated with this step is 1.08. This is somewhat lower than the value we measured at 700 Pa water, but is similar to low values previously reported using higher water pressures (21, 28).

The involvement of weakly adsorbed water in multiple mechanistic steps is also consistent with the large reaction order (1.3). DFT calculations also indicate that a second adsorbed water molecule in the vicinity of the  $^{*}\text{COOH}$  species facilitates the proton transfer, which only needs to overcome the thermodynamic barrier ( $\Delta E = 0.70$  eV,  $E_a = 0.70$  eV, SM 6.6). Further, at higher water coverage, rapid proton mobility (33) can explain the shift to an equilibrium isotope effect. We also note that  $^{*}\text{COOH}$  decomposition has been identified as the RDS in the related water-gas shift reaction on Cu and Pt (34, 35), and that this is consistent with reports of NaOH promoting CO oxidation over Au catalysts. (17, 36)

The CO oxidation mechanism shown in Fig. 4, along with the structural model of support OH groups anchoring and activating water near Au particles, provide a fresh framework for interpreting previous results. This model provides a single active site description that unifies some very disparate mechanistic information, accounts for the promotional effects of water, and is consistent with previously reported isotope exchange studies (21, 27) that indicate that CO and O<sub>2</sub> must react directly on the Au particles without exchanging O atoms with the support or adsorbed water. At the same time, it maintains the importance of the support OH groups and the metal-support interface without directly involving them in the reaction mechanism. The likely active sites bear a strong resemblance to the WGS mechanism over Au catalysts, where the support anchors water near Au-CO sites (6).

This proposed mechanism explains why the O<sub>2</sub> adsorption and activation steps, which are widely regarded as the critical mechanistic steps, have been so difficult to characterize. The fast room-temperature catalysis mechanism requires both water and CO for O<sub>2</sub> binding and activation. Experiments performed without water, particularly UHV and DFT studies, ultimately probe different reaction mechanisms than what appears to be the dominant room temperature pathway on supported catalysts. Similarly, most traditional catalyst studies rarely control or report feed water contents, which has likely contributed to the wide range of reported CO oxidation activities for Au/TiO<sub>2</sub> catalysts, and to the difficulties in understanding the key features of the best catalysts. Finally,

this new mechanism brings the interpretation of traditional supported catalyst experiments more in line with computational and surface science studies, which have largely indicated that the key reaction steps occur on Au (7, 9–14, 17, 29), without direct participation of the support.

## References and Notes

- M. Carguello, V. V. Doan-Nguyen, T. R. Gordon, R. E. Diaz, E. A. Stach, R. J. Gorte, P. Fornasiero, C. B. Murray, Control of metal nanocrystal size reveals metal-support interface role for ceria catalysts. *Science* **341**, 771–773 (2013). [Medline doi:10.1126/science.1240148](#)
- A. Corma, P. Serna, Chemoselective hydrogenation of nitro compounds with supported gold catalysts. *Science* **313**, 332–334 (2006). [Medline doi:10.1126/science.1128383](#)
- T. Takei, T. Akita, I. Nakamura, T. Fujitani, M. Okumura, K. Okazaki, J. Huang, T. Ishida, M. Haruta, Heterogeneous catalysis by gold. *Adv. Catal.* **55**, 1–126 (2012). [doi:10.1016/B978-0-12-385516-9.00001-6](#)
- B. N. Zope, D. D. Hibbitts, M. Neurock, R. J. Davis, Reactivity of the gold/water interface during selective oxidation catalysis. *Science* **330**, 74–78 (2010). [Medline doi:10.1126/science.1195055](#)
- C. Della Pina, E. Faletta, M. Rossi, Update on selective oxidation using gold. *Chem. Soc. Rev.* **41**, 350–369 (2012). [Medline doi:10.1039/c1cs15089h](#)
- M. Shekhar, J. Wang, W. S. Lee, W. D. Williams, S. M. Kim, E. A. Stach, J. T. Miller, W. N. Delgass, F. H. Ribeiro, Size and support effects for the water-gas shift catalysis over gold nanoparticles supported on model Al<sub>2</sub>O<sub>3</sub> and TiO<sub>2</sub>. *J. Am. Chem. Soc.* **134**, 4700–4708 (2012). [Medline doi:10.1021/ja210083d](#)
- M. Valden, X. Lai, D. W. Goodman, Onset of catalytic activity of gold clusters on titania with the appearance of nonmetallic properties. *Science* **281**, 1647–1650 (1998). [Medline doi:10.1126/science.281.5383.1647](#)
- A. A. Herzing, C. J. Kiely, A. F. Carley, P. Landon, G. J. Hutchings, Identification of active gold nanoclusters on iron oxide supports for CO oxidation. *Science* **321**, 1331–1335 (2008). [Medline doi:10.1126/science.1159639](#)
- M. S. Chen, D. W. Goodman, The structure of catalytically active gold on titania. *Science* **306**, 252–255 (2004). [Medline doi:10.1126/science.1102420](#)
- H. Falsig, B. Hvolbaek, I. S. Kristensen, T. Jiang, T. Bligaard, C. H. Christensen, J. K. Nørskov, Trends in the catalytic CO oxidation activity of nanoparticles. *Angew. Chem. Int. Ed.* **47**, 4835–4839 (2008). [Medline doi:10.1002/anie.200801479](#)
- C. Lemire, R. Meyer, S. Shaikhutdinov, H.-J. Freund, Do quantum size effects control CO adsorption on gold nanoparticles? *Angew. Chem. Int. Ed.* **43**, 118–121 (2004). [Medline doi:10.1002/anie.200352538](#)
- G. Mills, M. S. Gordon, H. Metiu, Oxygen adsorption on Au clusters and a rough Au(111) surface. The role of surface flatness, electron confinement, excess electrons, and band gap. *J. Chem. Phys.* **118**, 4198 (2003). [doi:10.1063/1.1542879](#)
- I. N. Remediakis, N. Lopez, J. K. Nørskov, CO oxidation on rutile-supported au nanoparticles. *Angew. Chem. Int. Ed.* **44**, 1824–1826 (2005). [Medline doi:10.1002/anie.200461699](#)
- L. M. Molina, M. D. Rasmussen, B. Hammer, Adsorption of O<sub>2</sub> and oxidation of CO at Au nanoparticles supported by TiO<sub>2</sub>(110). *J. Chem. Phys.* **120**, 7673–7680 (2004). [Medline doi:10.1063/1.1687337](#)
- R. A. Ojifinni, N. S. Froemming, J. Gong, M. Pan, T. S. Kim, J. M. White, G. Henkelman, C. B. Mullins, Water-enhanced low-temperature CO oxidation and isotope effects on atomic oxygen-covered Au(111). *J. Am. Chem. Soc.* **130**, 6801–6812 (2008). [Medline doi:10.1021/ja800351j](#)
- D. Widmann, R. J. Behm, Activation of molecular oxygen and the nature of the active oxygen species for CO oxidation on oxide supported Au catalysts. *Acc. Chem. Res.* **47**, 740–749 (2014). [Medline doi:10.1021/ar400203e](#)
- M. S. Ide, R. J. Davis, The important role of hydroxyl on oxidation catalysis by gold nanoparticles. *Acc. Chem. Res.* **47**, 825–833 (2014). [Medline doi:10.1021/ar4001907](#)
- I. X. Green, W. Tang, M. Neurock, J. T. Yates Jr., Spectroscopic observation of dual catalytic sites during oxidation of CO on a Au/TiO<sub>2</sub> catalyst. *Science* **333**, 736–739 (2011). [Medline doi:10.1126/science.1207272](#)
- T. Fujitani, I. Nakamura, Mechanism and active sites of the oxidation of CO over Au/TiO<sub>2</sub>. *Angew. Chem. Int. Ed.* **50**, 10144–10147 (2011). [Medline doi:10.1002/anie.201104694](#)
- M. Daté, M. Okumura, S. Tsubota, M. Haruta, Vital role of moisture in the catalytic activity of supported gold nanoparticles. *Angew. Chem. Int. Ed.* **43**, 2129–2132 (2004). [Medline doi:10.1002/anie.200453796](#)
- M. Ojeda, B.-Z. Zhan, E. Iglesia, Mechanistic interpretation of CO oxidation turnover rates on supported Au clusters. *J. Catal.* **285**, 92–102 (2012). [doi:10.1016/j.jcat.2011.09.015](#)
- M. C. Kung, R. J. Davis, H. H. Kung, Understanding Au-catalyzed low-temperature CO oxidation. *J. Phys. Chem. C* **111**, 11767–11775 (2007). [doi:10.1021/jp072102i](#)
- M. Haruta, Spiers Memorial Lecture. Role of perimeter interfaces in catalysis by gold nanoparticles. *Faraday Discuss.* **152**, 11–32, discussion 99–120 (2011). [Medline doi:10.1039/c1fd00107h](#)
- J. A. Singh, S. H. Overbury, N. J. Dudney, M. Li, G. M. Veith, Gold nanoparticles supported on carbon nitride: Influence of surface hydroxyls on low temperature carbon monoxide oxidation. *ACS Catal.* **2**, 1138–1146 (2012). [doi:10.1021/cs3001094](#)
- W. C. Ketchie, M. Murayama, R. J. Davis, Promotional effect of hydroxyl on the aqueous phase oxidation of carbon monoxide and glycerol over supported Au catalysts. *Top. Catal.* **44**, 307–317 (2007). [doi:10.1007/s11244-007-0304-x](#)
- H. H. Kung, M. C. Kung, C. K. Costello, Supported Au catalysts for low temperature CO oxidation. *J. Catal.* **216**, 425–432 (2003). [doi:10.1016/S0021-9517\(02\)00111-2](#)
- J. T. Calla, R. J. Davis, Oxygen-exchange reactions during CO oxidation over titania- and alumina-supported Au nanoparticles. *J. Catal.* **241**, 407–416 (2006). [doi:10.1016/j.jcat.2006.05.017](#)
- C. K. Costello, J. H. Yang, H. Y. Law, Y. Wang, J.-N. Lin, L. D. Marks, M. C. Kung, H. H. Kung, On the potential role of hydroxyl groups in CO oxidation over Au/Al<sub>2</sub>O<sub>3</sub>. *Appl. Catal. A* **243**, 15–24 (2003). [doi:10.1016/S0926-860X\(02\)00533-1](#)
- S. Laursen, S. Linic, Geometric and electronic characteristics of active sites on TiO<sub>2</sub>-supported Au nano-catalysts: Insights from first principles. *Phys. Chem. Chem. Phys.* **11**, 11006–11012 (2009). [Medline doi:10.1039/b912641d](#)
- J. Carrasco, A. Hodgson, A. Michaelides, A molecular perspective of water at metal interfaces. *Nat. Mater.* **11**, 667–674 (2012). [Medline doi:10.1038/nmat3354](#)
- C. G. Long, J. D. Gilbertson, G. Vijayaraghavan, K. J. Stevenson, C. J. Pursell, B. D. Chandler, Kinetic evaluation of highly active supported gold catalysts prepared from monolayer-protected clusters: An experimental Michaelis-Menten approach for determining the oxygen binding constant during CO oxidation catalysis. *J. Am. Chem. Soc.* **130**, 10103–10115 (2008). [Medline doi:10.1021/ja801279a](#)
- Z.-P. Liu, P. Hu, A. Alavi, Catalytic role of gold in gold-based catalysts: A density functional theory study on the CO oxidation on gold. *J. Am. Chem. Soc.* **124**, 14770–14779 (2002). [Medline doi:10.1021/ja0205885](#)
- L. R. Merte, G. Peng, R. Bechstein, F. Rieboldt, C. A. Farberow, L. C. Grabow, W. Kudernatsch, S. Wendt, E. Lægsgaard, M. Mavrikakis, F. Besenbacher, Water-mediated proton hopping on an iron oxide surface. *Science* **336**, 889–893 (2012). [Medline doi:10.1126/science.1219468](#)
- A. A. Gokhale, J. A. Dumesic, M. Mavrikakis, On the mechanism of low-temperature water gas shift reaction on copper. *J. Am. Chem. Soc.* **130**, 1402–1414 (2008). [Medline doi:10.1021/ja0768237](#)
- L. C. Grabow, A. A. Gokhale, S. T. Evans, J. A. Dumesic, M. Mavrikakis, Mechanism of the water gas shift reaction on pt: first principles, experiments, and microkinetic modeling. *J. Phys. Chem. C* **112**, 4608–4617 (2008). [doi:10.1021/jp7099702](#)
- G. M. Veith, A. R. Lupini, N. J. Dudney, Role of pH in the formation of structurally stable and catalytically active TiO<sub>2</sub>-supported gold catalysts. *J. Phys. Chem. C* **113**, 269–280 (2009). [doi:10.1021/jp808249f](#)

## Supplementary Materials

[www.sciencemag.org/cgi/content/full/science.1256018/DC1](http://www.sciencemag.org/cgi/content/full/science.1256018/DC1)

Materials and Methods

Supplementary Text

Figs. S1 to S12

Scheme S1

Tables S1 to S8

Movie S1

13 May 2014; accepted 8 August 2014  
Published online 4 September 2014  
10.1126/science.1256018

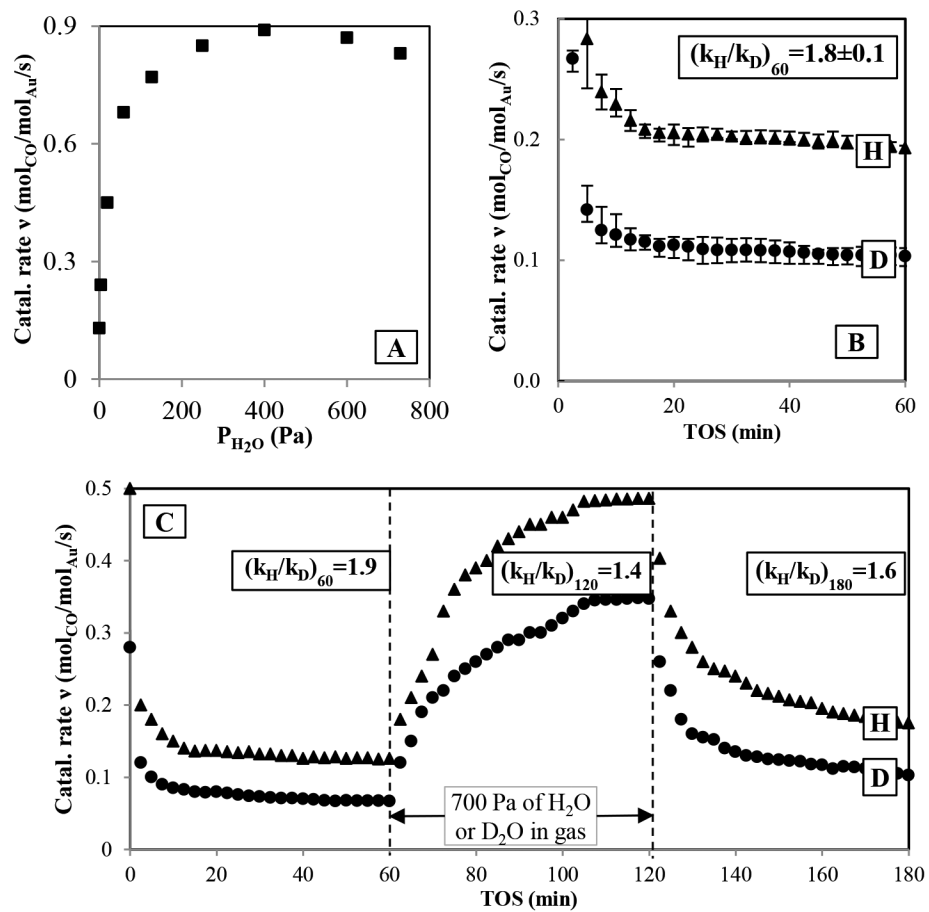


**Fig. 1. Water and kinetic isotopic effects on CO oxidation over Au/TiO<sub>2</sub> (20°C, 1% CO, 20% O<sub>2</sub>, SV = 36 L/g catalyst/min).** (A) Effects of water on the overall reaction rate. (B) Reaction rate for protonated ( $\blacktriangle$ **H**) and deuterated ( $\blacksquare$ **D**) catalysts in the absence of added water (6 trials averaged). (C) Changes in reaction rate induced by adding 700 Pa of H<sub>2</sub>O/D<sub>2</sub>O.

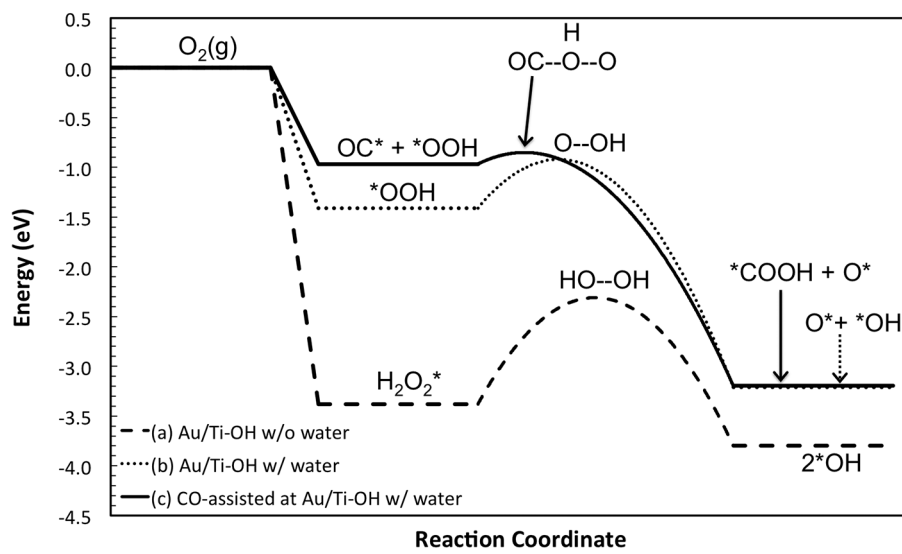


**Fig. 2. Potential energy diagrams for O<sub>2</sub> binding and O-O bond activation near the Au/TiO<sub>2</sub> interface.** (a) In the absence of H<sub>2</sub>O (dashed pathway), O<sub>2</sub> adsorption at the Au/TiO<sub>2</sub> interface initiates a spontaneous transfer of two protons, forming H<sub>2</sub>O<sub>2</sub><sup>\*</sup>; (b) With an adsorbed H<sub>2</sub>O (dotted pathway), O-O bond activation leads preferentially to O\* and \*OH; (c) With adsorbed H<sub>2</sub>O and CO (solid pathway), O-O scission is facilitated by nucleophilic attack of \*CO, resulting in \*COOH (carboxyl).

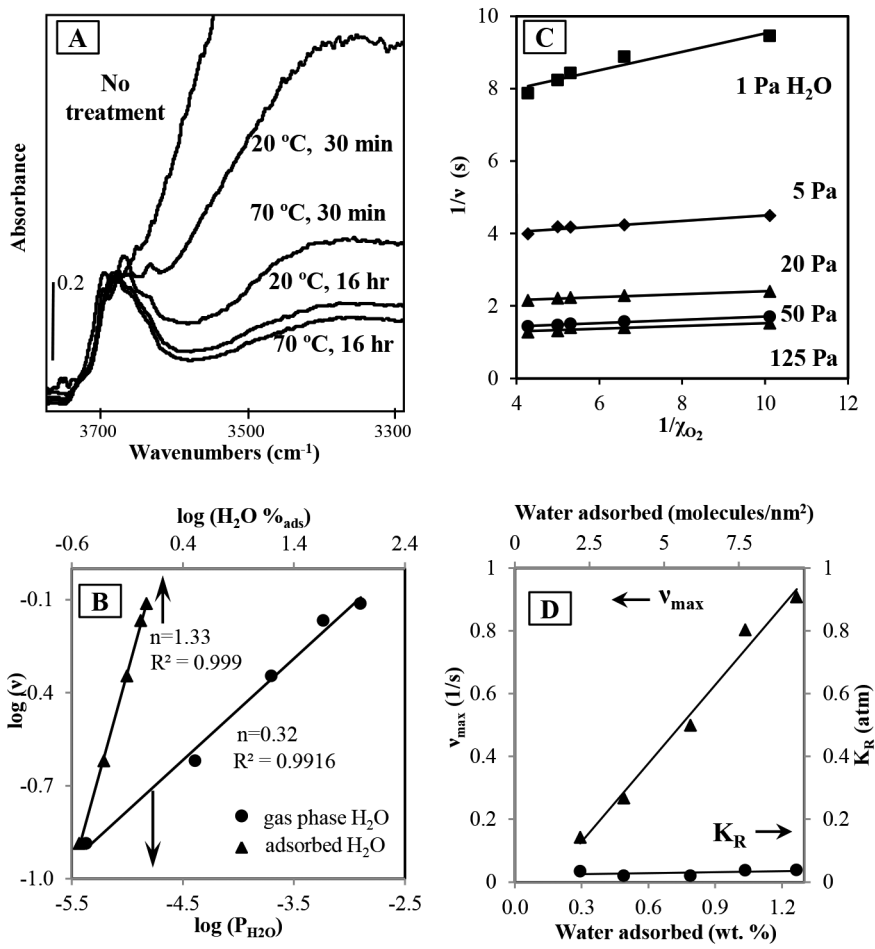


**Fig. 3.** (A) IR spectra and catalytic activity for gently dried catalysts. (B) Reaction order based on gas phase (●) and weakly adsorbed (▲) water (20°C, 1% CO, SV = 35 L/g catalyst/min). (C) Double reciprocal plots used in Michaelis-Menten kinetic treatment. (D) Michaelis-Menten kinetic parameters vs. catalyst water content.

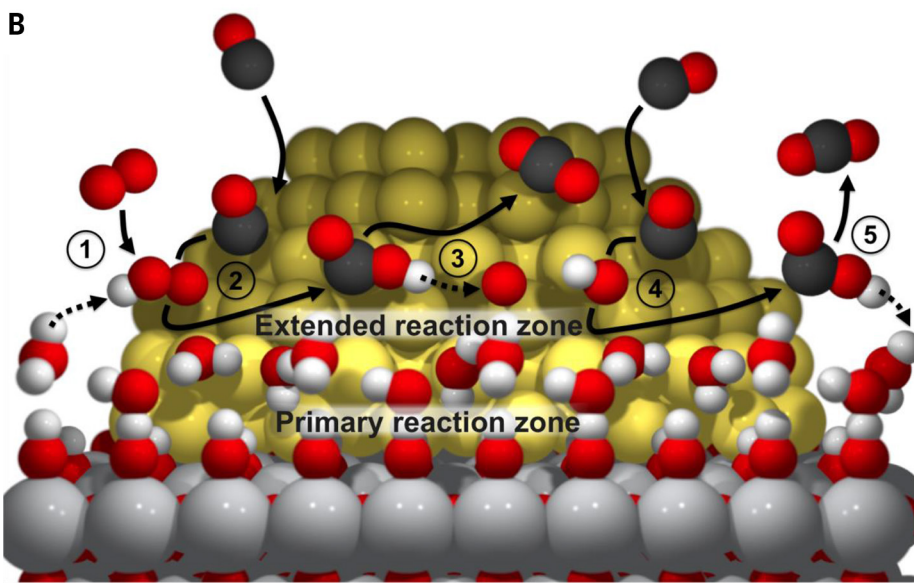
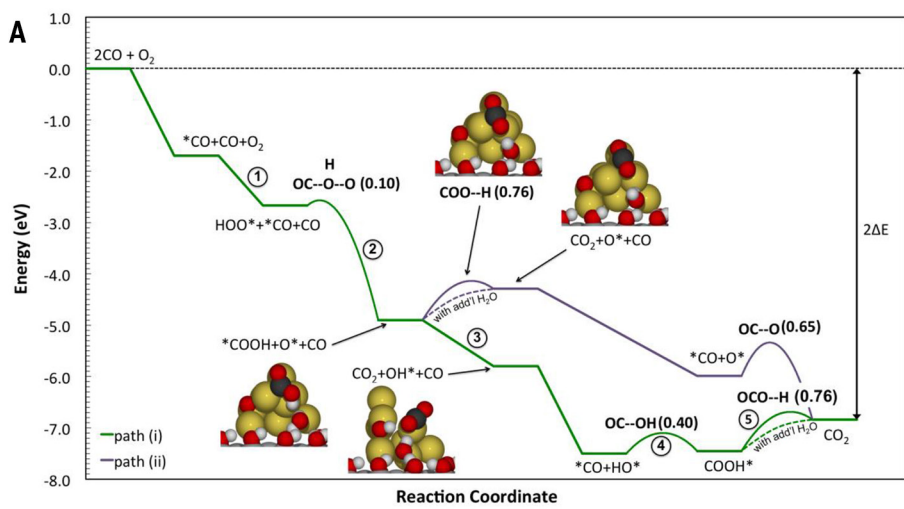


**Fig. 4. Proposed reaction mechanism.** (A) Potential energy diagram; both pathways are limited by a combination of \*COOH decomposition and the reaction between \*CO and \*O(H). (B) Schematic representation of the lower (green) pathway.

**Table 1. Effects of drying treatments on IR spectra and catalytic activity.**

Drying treatment <sup>1</sup>	Ti-OH Area <sup>2</sup>	H <sub>2</sub> O Area <sup>3</sup>	ν (s <sup>-1</sup> )
None	14.3	841.7	0.32
20°C, ½ hour	14.1	503.0	0.22
70°C, ½ hour	14.0	227.5	0.18
20°C, 16 hours	13.9	131.3	0.09
70°C, 16 hours	13.8	102.2	0.03

<sup>1</sup>N<sub>2</sub> flowing at 50 mL/min<sup>2</sup>3741-3545 cm<sup>-1</sup><sup>3</sup>3800-1800 cm<sup>-1</sup>